CHAPTER 5

MODEL EVALUATION

5.1 Flow Pattern Predictions

The model prediction results and experimental data are plotted on flow pattern maps using superficial gas and liquid velocities as coordinates. **Figs. 5-1** through **5-6** display the flow patterns of nitrogen and water two-phase flow at the inclination angle of 0, 1, and 3 degrees, respectively, predicted for 106. 4 mm i.d. pipes at 35±5° temperature and low (592 kPa) and high (2060 kPa) pressures. The lines in figures represent model prediction results while the points represent experimental data. The agreement between model prediction and experimental data is very good.

The model prediction for the transition from intermittent to dispersed-bubble flow is based on the concept of bubble size proposed by Barea *et al.*[1] The applicability of two critical bubble sizes, d_{CB} and d_{CD}, were first evaluated. **Figs. 5-1** through **5-6**, depict the boundary by the broken lines estimated with the criterion $d_{max}= d_{CB}$, and the solid lines estimated with $d_{max}=d_{CD}$. On the experimental conditions of low and high pressures, d_{CB} is smaller than d_{CD}. In vertical or high inclination flow, the criterion $d_{max}=d_{CD}$ is usually effective, while the criterion $d_{max}= d_{CB}$ is effective in horizontal or slightly inclined flow. It is seen in the figures for the high pressure that the broken lines obtained by the criterion $d_{max}= d_{CB}$ are located within the dispersed-bubble flow region, and that the solid lines based on $d_{max}=d_{CD}$, partially go through the intermittent flow region. However, since the flow patterns identified as transitional flow resemble dispersed-bubble flow more closely than intermittent flow, it is more appropriate to apply only the criterion $d_{max}=d_{CD}$ in model calculations for all the inclination angles. This criterion showed good coincidence nature with experiment data at both low and high pressure conditions. This transition is insensitive to the angle of inclination and relatively insensitive to pressure in pipe.

For prediction of stratified and non-stratified flow transition, we used the Bendiksen and Espedal[2] criterion in addition to the Taitel and Dukler[3] criterion. The latter demonstrates good

agreements with the experimental data of small diameter and low-pressure conditions[4]. At large diameter conditions in this study, the Bendiksen and Espedal boundary moves to higher liquid superficial velocity because slug translational velocity depends on the pipe diameter (Eq. 4-21). The Taitel and Dukler boundary is relatively insensitive to the pipe diameters, though it is very effective in the large diameter case.

The results stated above show that to use simultaneously Bendiksen and Espedal criterion and Taitel and Dukler criterion is more effective on all conditions.

For prediction of stratified and non-stratified flow transition, the dimensionless liquid level, h_L/d, is an important parameter. Since the interfacial friction factor between gas and liquid affects greatly on the liquid level, it is very important to use a correct interfacial friction factor. In this study, f_I = 0.0142 (Eq. (4-16)) was used to low-pressure conditions, and f_I = 0.022 (Eq. (4-17)) was used to high-pressure conditions. Because this transition is sensitive to the flow pressure that directly affects density of gas, it is thought that the interfacial friction factor is larger at high-pressure conditions.

The stratified and non-stratified flow boundary was found most sensitive to the inclination angle that causes the liquid to move slower with higher liquid holdups and prevents stratification. However, with higher superficial gas velocity with relatively low superficial liquid velocity in the case of 1° inclination, stratified roll-wave (SR) flow was observed in low-pressure experiments (see **Fig. 5-3**), and predicted correctly by the model. It is to be noted that only the stratified roll wave (SR) region appeared at high gas rates with low liquid rates for the slightly inclined cases as seen in **Figs. 5-3** and **5-4**. At high-pressure conditions, the whole range of stratified flow was detected by liquid holdup at the tested conditions (see **Fig. 5-2**), though the flow cannot be visually observed for high pressures. It was difficult to determine the difference between stratified-wave and stratified-roll-wave only by the holdup sensor signals.

The intermittent flow pattern is subdivided into the elongate-bubble, slug, and froth flow based on the experimental data. The pattern classified as froth flow is not a flow type like churn or froth flow in vertical or high inclination pipes, but a type of slug flow with a higher gas rate that causes liquid slugs split in gas plugs. Model predictions of these three flow patterns were

performed on the basis of the average liquid level, and showed good agreements with the data.

Most of the intermittent flow were identified as the elongated-bubble and slug flow, and matched well by model predictions. At low-pressure experiments, elongated-bubble flow was not observed on the tested range of the flow conditions. In high-pressure experiments, the most notable difference from the small diameter and low-pressure case[4)] is that the elongated-bubble region is transitional directly to the dispersed-bubble region. The experimental results identified as the froth flow were also reasonably matched with model predictions.

Transition from annular to intermittent flow occurs when instability of annular flow prevents a stable annular configuration. Annular flow is generally observed in horizontal and near horizontal pipes at low-pressure conditions. In this case, most of the wavy liquid stays at the bottom of the pipe while only a small amount of liquid sweeps around to wet the pipe with a thin film (see **Fig. 2-4 (b)**). With the rate of liquid flow increased, waves of finite amplitude begin to grow. As a result of the suction over the crest of the wave, liquid must be supplied from the fluid in the film adjacent to the wave, and waves develops into frothy waves. If the liquid level becomes above the certain level, the peak of the frothy wave will reach the top before the trough reaches the bottom of the pipe, and froth flow results. Based on experiment data, we evaluated the liquid level $h_L/d = 0.25$ as the transition boundary. If liquid level, $h_L/d > 0.45$, slug or dispersed bubble flow will be resulted in. Results of these criterions are shown in **Figs. 5-1** through **5-3**.

At high-pressure experiments, the results of model prediction did not show annular flow in the range of the tested conditions. In experiments, however, three data points as marked by unfilled square in **Figs. 5-2** and **5-4** showed transitional behavior between the stratified and annular flow as shown in **Fig. 3-18**. The model predicted that those are located on or close to the boundary between the stratified roll-wave and annular region.

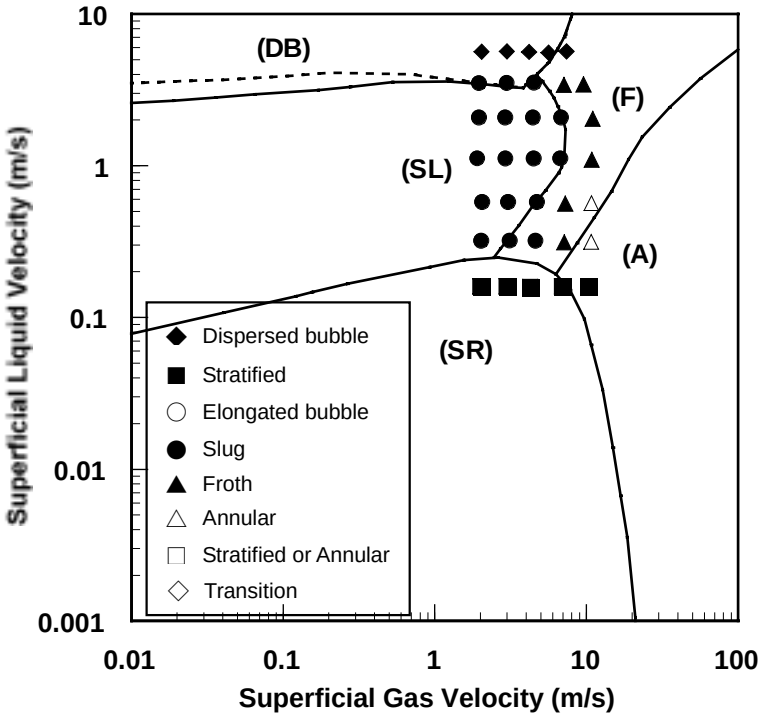

Fig. 5-1 Flow Pattern Map for Nitrogen-Water System in 106. 4 mm ID, Horizontal Pipe at Low-Pressure (592 kPa)

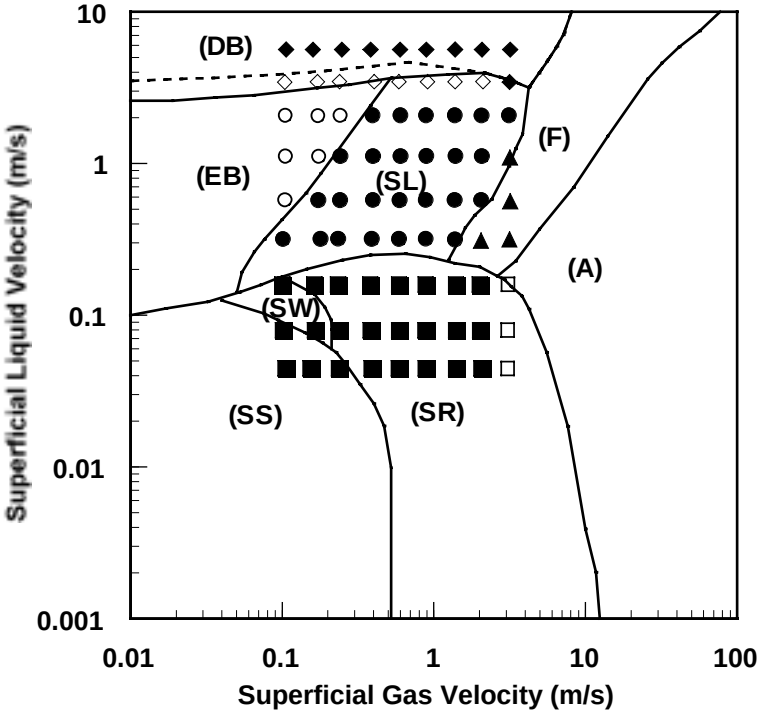

Fig. 5-2 Flow Pattern Map for Nitrogen-Water System in 106. 4 mm ID, Horizontal Pipe at High-Pressure (2060 kPa)

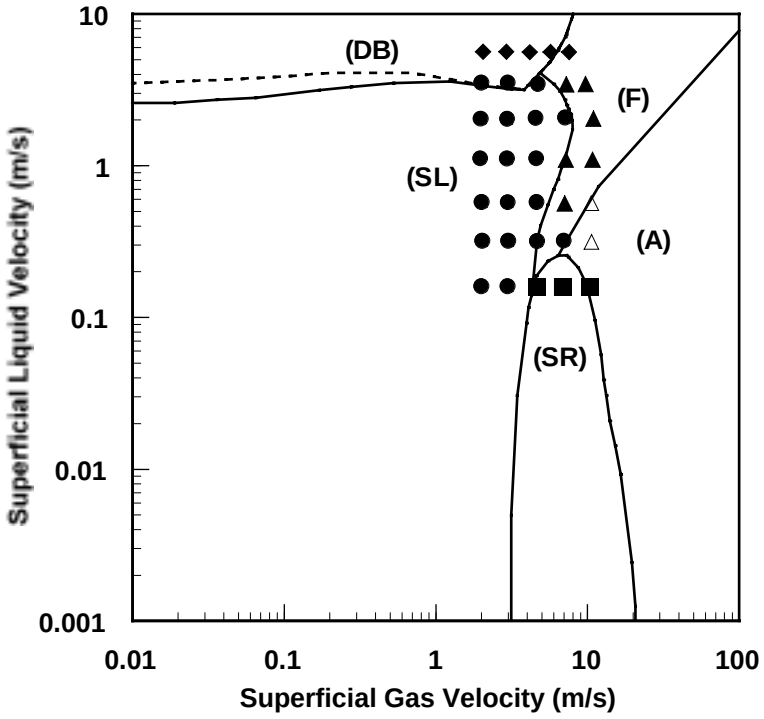

Fig. 5-3 Flow Pattern Map for Nitrogen-Water System in 106. 4 mm ID, 1° Inclined Pipe at Low-Pressure (592 kPa)

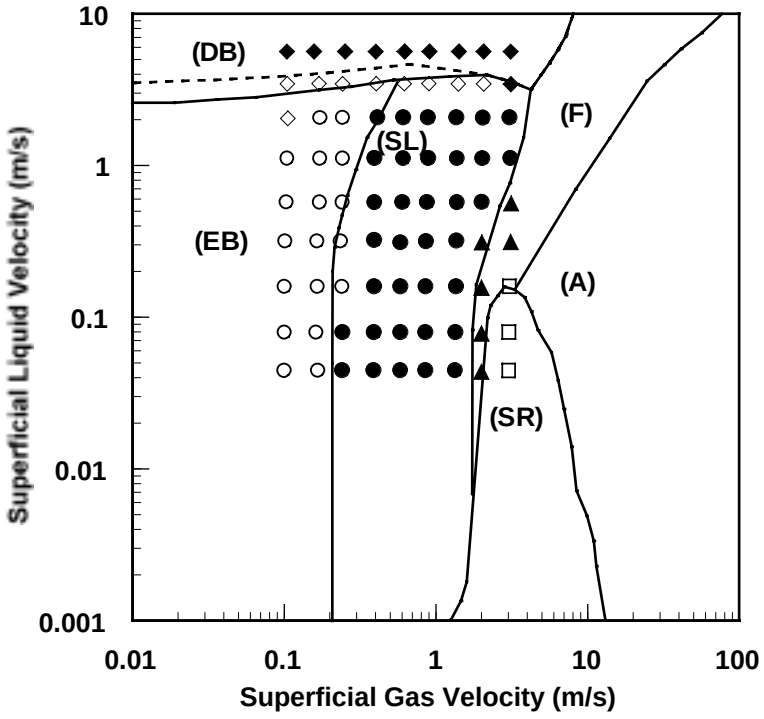

Fig. 5-4 Flow Pattern Map for Nitrogen-Water System in 106. 4 mm ID, 1° Inclined Pipe at High-Pressure (2060 kPa)

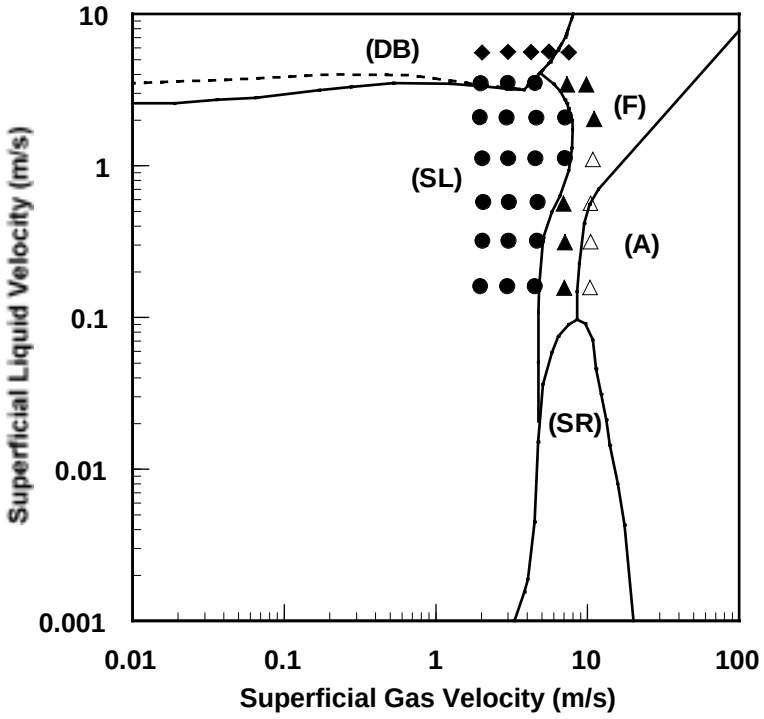

Fig. 5-5 Flow Pattern Map for Nitrogen-Water System in 106. 4 mm ID, 3° Inclined Pipe at Low-Pressure (592 kPa)

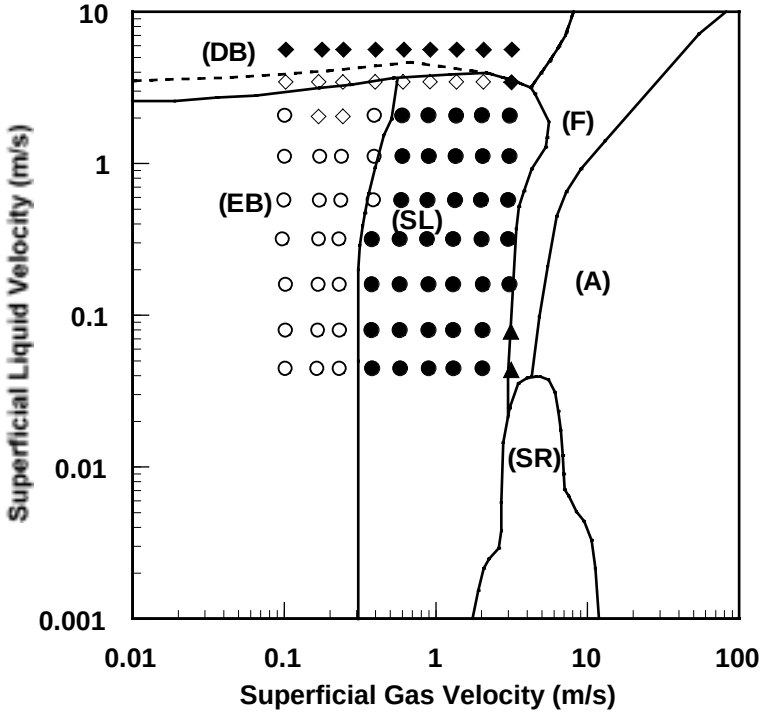

Fig. 5-6 Flow Pattern Map for Nitrogen-Water System in 106. 4 mm ID, 3° Inclined Pipe at High-Pressure (2060 kPa)

5.2 Statistical Parameters

Three statistical parameters, i.e. average percentage error, absolute average percentage error, and standard deviation were used to evaluate the predictions of proposed model for liquid holdup and pressure drops.

$$\varepsilon_1 = (\sum_{i=1}^{n} e_i) / n \quad \text{(Average percentage error)} \tag{5-1}$$

$$\varepsilon_2 = (\sum_{i=1}^{n} |e_i|) / n \quad \text{(Absolute average percentage error)} \tag{5-2}$$

$$\varepsilon_3 = (\sum_{i=1}^{n} (e_i - \varepsilon_1)^2)^{1/2} /(n-1)^{1/2} \quad \text{(Standard deviation)} \tag{5-3}$$

where n is the total number of data points, and the relative error, e_i, is given by

$$e_i = ((\Delta p_i)_C - (\Delta p_i)_M) \times 100 /(\Delta p_i)_M \tag{5-4}$$

The average percentage error, ε_1, is a measure of degree of the over-prediction (positive value) or under-prediction (negative value). The absolute percentage error, ε_2, is a measure of the agreement between the predicted and measured value. The standard deviation, ε_3, indicates the scatter of the error with respect to the corresponding average error.

5.3 Liquid Holdup Predictions

Based on the flow patterns predicted, liquid holdup was calculated for the individual flow conditions of the experiments. Comparisons between the predictions by the proposed model and the experimental data for the average liquid holdup of each flow pattern are presented and evaluated in the following sections. Error analysis results are listed in **Table 5-1**.

Table 5-1 Accuracy Evaluation of Liquid Holdup

Flow patterns	Average error ε_1 [%]	Absolute average error, ε_2 [%]	Standard deviation, ε_3	Number of data
Low-pressure				
Dispersed bubble	1.65	3.77	4.84	18
Stratified	-5.11	11.94	15.28	6
Intermittent	-14.26	14.91	10.68	75
Annular	87.09	87.09	25.94	6
All patterns	-5.22	16.96	26.22	105
High-pressure				
Dispersed bubble	-1.13	1.77	2.40	54
Stratified	-2.33	3.03	19.59	30
Intermittent	-1.20	5.96	9.33	159
All patterns	-2.56	6.28	10.25	243

5.3.1 Dispersed Bubble Flow

The performance of the model for dispersed bubble flow of all inclination angles is shown in **Fig. 5-7**.

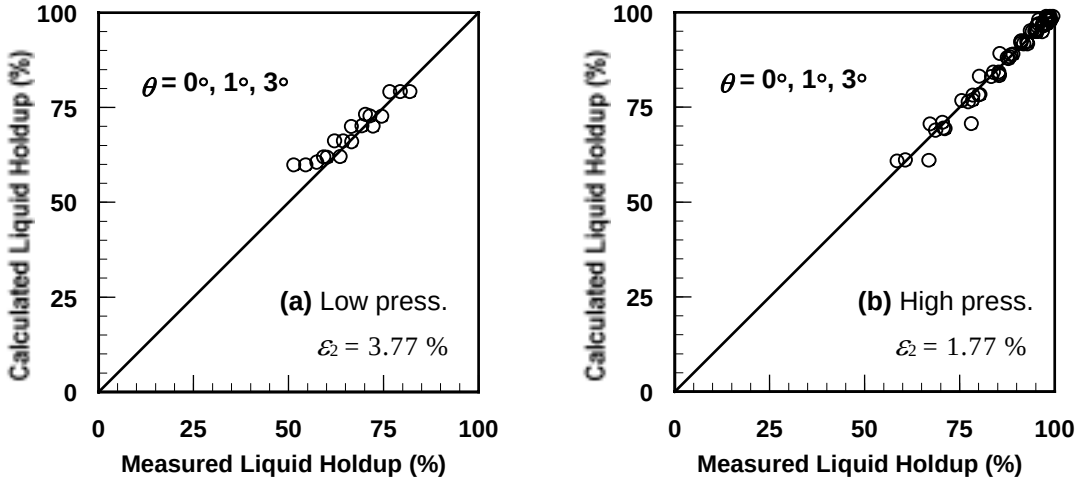

Fig. 5-7 Accuracy of Liquid Holdup Calculations for Dispersed Bubble Flow

Fig. 5-7 (a) shows a comparison between the predicted and measured liquid holdup of 18 data points for the low-pressure conditions, and **Fig. 5-7 (b)** shows 54 data points for the high-pressure conditions. The predictions of the proposed model show excellent agreements with these data sets, with 1.65 % average error, 3.77 % absolute average error, and 4.84 standard deviation for low-pressure conditions, and with -1.13 % average error, 1.77 % absolute average

error, and 2.40 standard deviation for high-pressure conditions. The slip model was found more effective to improve accuracy for these experimental conditions. **Figs. 5-8** through **5-10** show comparisons between the slip and non-slip models with the measured liquid holdup at low and high pressure conditions for the inclination angle 0°, 1°, and 3°, respectively. The liquid holdup is graphed against the gas flow rate. The liquid velocity is set constant as v_{SL}=5.63 m/s for each inclination angle. In these figures, the broken line and solid line represent the low and high pressure experiments, respectively.

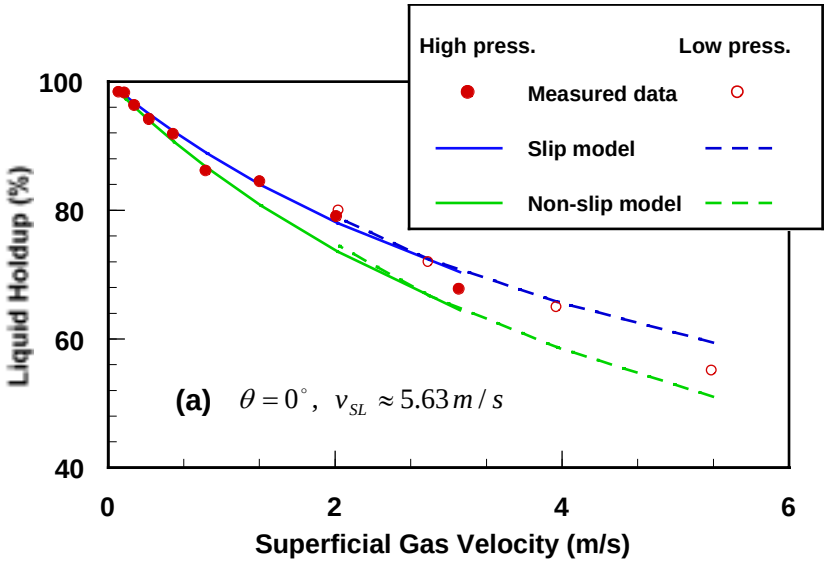

Fig. 5-8 Comparison of Slip and Non-Slip Models for Dispersed Bubble Flow, θ = 0°

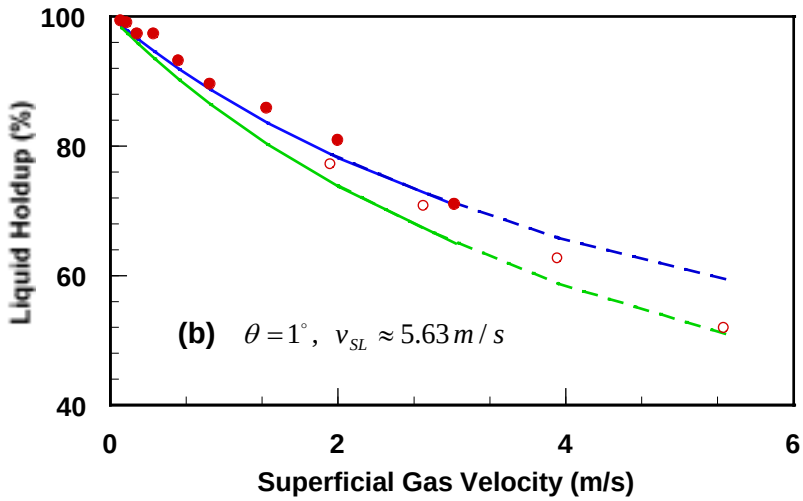

Fig. 5-9 Comparison of Slip and Non-Slip Models for Dispersed Bubble Flow, θ = 1°

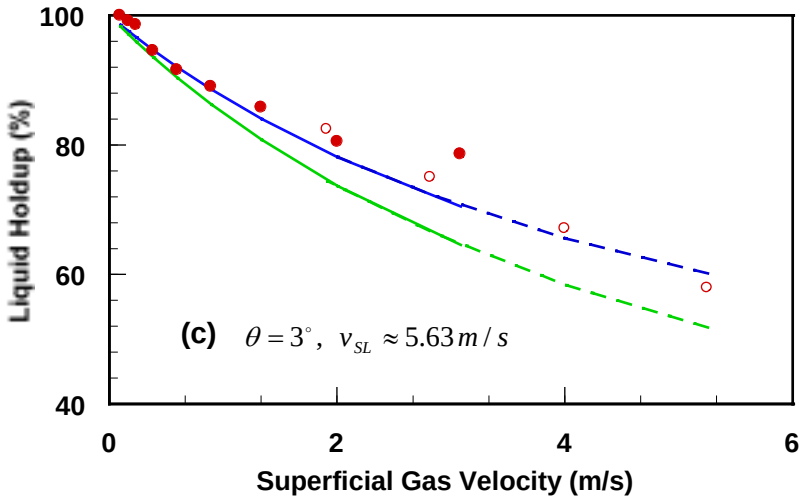

Fig. 5-10 Comparison of Slip and Non-Slip Models for Dispersed Bubble Flow, θ = 3°

5.3.2 Stratified Flow

The performance of the model for stratified flow of all inclination angles is shown in **Fig. 5-11**. The predicted model consists of stratified-smooth, stratified-wave, and stratified roll-wave flow patterns. For prediction of liquid holdup, we used the Lockhart and Mattinelli parameter, and performed estimation by implementing an appropriate fluid-wall friction factors as well as an interfacial friction factor to take into account the effects of different stratified flow patterns and inclination angle. **Fig. 5-11 (a)** shows a comparison between the predicted and measured liquid holdups of 6 data points for the low-pressure conditions, and **Fig. 5-11 (b)** shows 30 data points for the high-pressure conditions. The predictions of the proposed model show good agreements with this data set, with -5.11 % average error, 11.94 % absolute average error, and 15.28 standard deviation for low-pressure conditions, and with -2.33 % average error, 3.03 % absolute average error, and 19.59 standard deviation for high-pressure conditions.

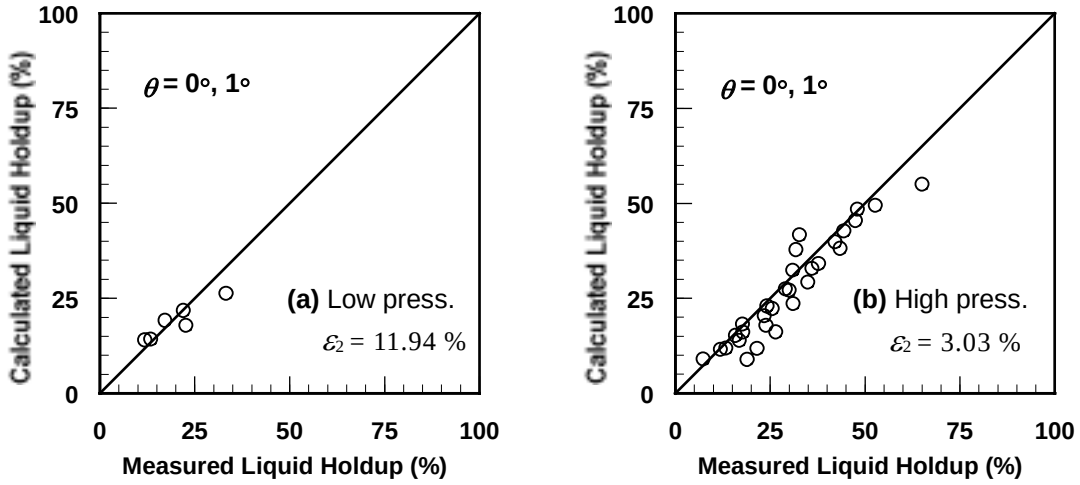

Fig. 5-11 Accuracy of Liquid Holdup Calculations for Stratified Flow

5.3.3 Intermittent Flow

The predicted model consists of elongated-bubble, slug, and froth flow patterns. The prediction model is based on the overall liquid mass balance over a slug unit. The elongated-bubble flow was treated the same as the slug flow in the model. For the froth flow, the slug model was applied assuming a constant value of the distribution parameter, C_o, for the translational velocity. The performances of the model for intermittent flow of each flow pattern and each inclination angle are shown in **Fig. 5-12** and **Fig. 5-13**, respectively. **Fig. 5-13 (a)** displays a comparison between the predicted and measured liquid holdup of 75 data points for the all inclination angles at low-pressure conditions, and **Fig. 5-13 (b)** shows 159 data points for the all inclination angles at high-pressure conditions. The predictions of the proposed model show good agreements with this data set, with -14.26 % average error, 14.91 % absolute average error, and 10.68 standard deviation for low-pressure conditions, and with -1.20 % average error, 5.96 % absolute average error, and 9.33 standard deviation for high-pressure conditions.

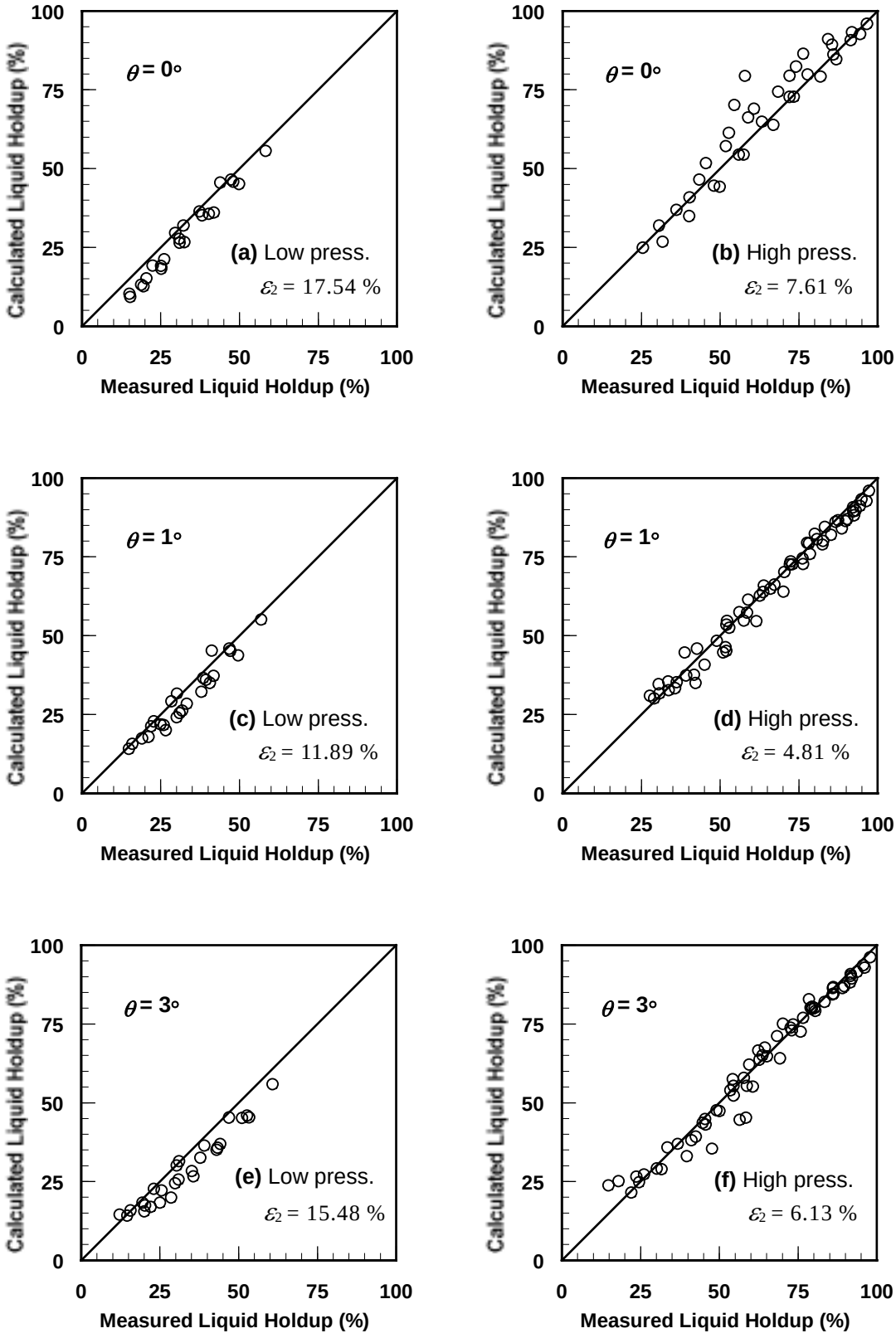

Fig. 5-12 Accuracy of Liquid Holdup Calculations for Intermittent Flow at Each Inclination Angle

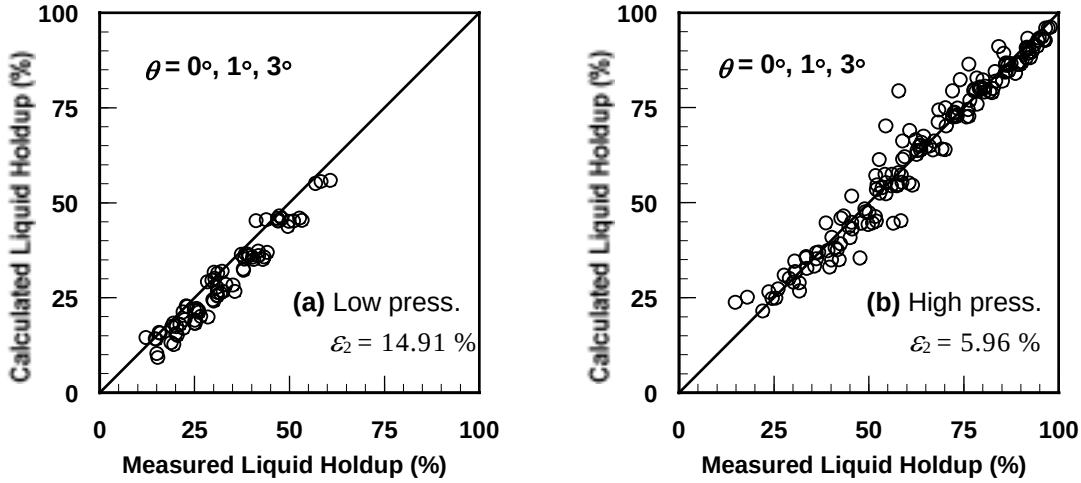

Fig. 5-13 Accuracy of Liquid Holdup Calculations for Intermittent Flow of All Inclination Angles

5.3.4 Annular Flow

Fig. 5-14 shows the model performance for annular flow comparing the computed results with the measured data for 6 points. Error analysis resulted in 87.09 % average error, 87.09 % absolute average error, and 25.94 standard deviation.

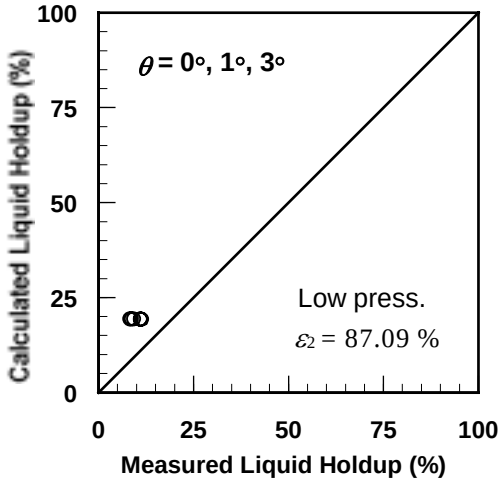

Fig. 5-14 Accuracy of Liquid Holdup Calculations for Annular Flow

The error analysis results are larger values than those of the other flow patterns. As seen in the

figure, the values of measurement show smaller values than calculations. The cause of this is that we used a conductance-type sensor for liquid holdup measurements in this study. This holdup sensor measures at flow conditions the volume ratio of the conductive fluid that accomplishes a continuous phase in multiphase flow in which one phase is a conductive fluid and the other phases are non-conductive fluids. In addition, because of the above principle, the holdup sensor cannot detect the conductive fluid isolated from the continuous phase, like the liquid drops which are entrained in the gas phase of annular flow. This point is one of the causes for error.

5.4 Pressure Drop Predictions

Each experimental run provides 3 pressure drop data at the10 m and 7.7 m sections and the whole length. Comparisons between the predictions by the proposed model and the experimental data for the pressure drop of individual flow patterns are presented and discussed in the following sections. The results of the pressure drop are listed for the individual flow pattern models in **Table 5-2**.

Table 5-2 Accuracy Evaluation of Pressure Drop

Flow patterns	Average error ε_1 [%]	Absolute average error, ε_2 [%]	Standard deviation, ε_3	Number of data
Low-pressure				
Dispersed bubble	3.85	12.28	14.72	54
Stratified	1.59	27.17	44.59	15
Intermittent	-4.40	16.13	21.81	195
Annular	-4.91	12.15	15.46	18
All patterns	-2.53	15.73	22.23	282
High-pressure				
Dispersed bubble	3.15	3.73	4.01	162
Stratified	-4.21	35.81	69.55	27
Intermittent	1.04	16.02	38.40	467
All patterns	1.34	13.80	35.31	656

5.4.1 Dispersed Bubble Flow

The performance of the model for dispersed bubble flow of all inclination angles is shown in

Fig. 5-15. **Fig. 5-15 (a)** shows a comparison between the predicted and measured pressure drops of 54 data points for low-pressure conditions. **Fig. 5-15 (b)** shows 162 data points for the high-pressure conditions. The performance of the model shows 3.85 % average error, 12.28 % absolute average error, and 14.72 standard deviation for low-pressure conditions, and 3.15 % average error, 3.73 % absolute average error, and 4.01 standard deviation for high-pressure conditions.

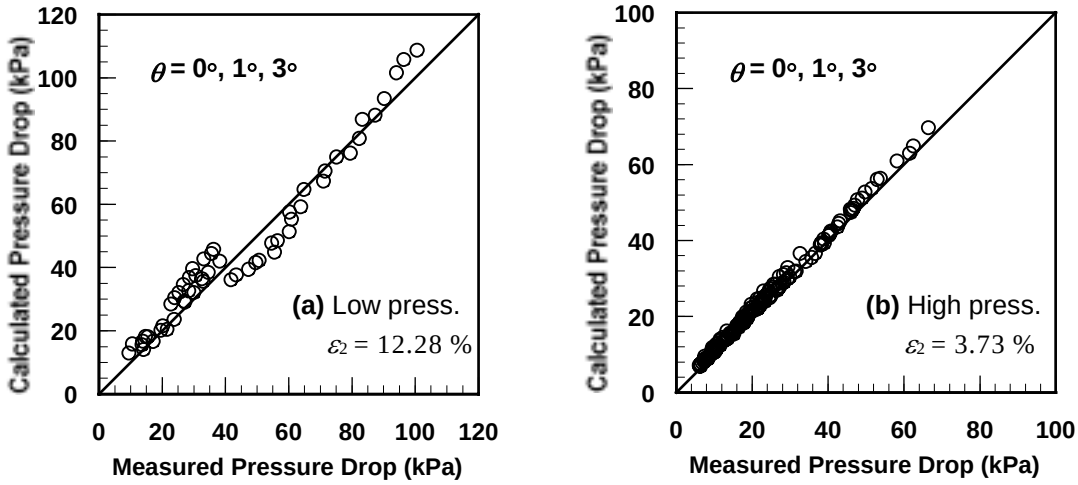

Fig. 5-15 Accuracy of Pressure Drop Calculations for Dispersed Bubble Flow

5.4.2 Stratified Flow

Figs. 5-16 (a), **(b**) and **(c)** display comparisons between the model calculations and measured pressure drops for the stratified flow with increasing the gas flow rate and constant liquid velocities, v_{SL}=0.044 m/s, 0.078 m/s, and 0.156 m/s, respectively, at horizontal case. As seen in the figures, the experimental runs of stratified flow generated much lower pressure drops than those of the other flow patterns. On these experimental conditions, it was difficult to obtain correct data for low gas and low liquid stratified flow due to the resolution limit of the pressure transducers. Pressure drops were close to zero when superficial gas velocity was lower than 0.5 m/s with low liquid rates. Nevertheless, as shown in the figures, the predicted results show good agreements with the experimental data as the superficial gas velocity increases.

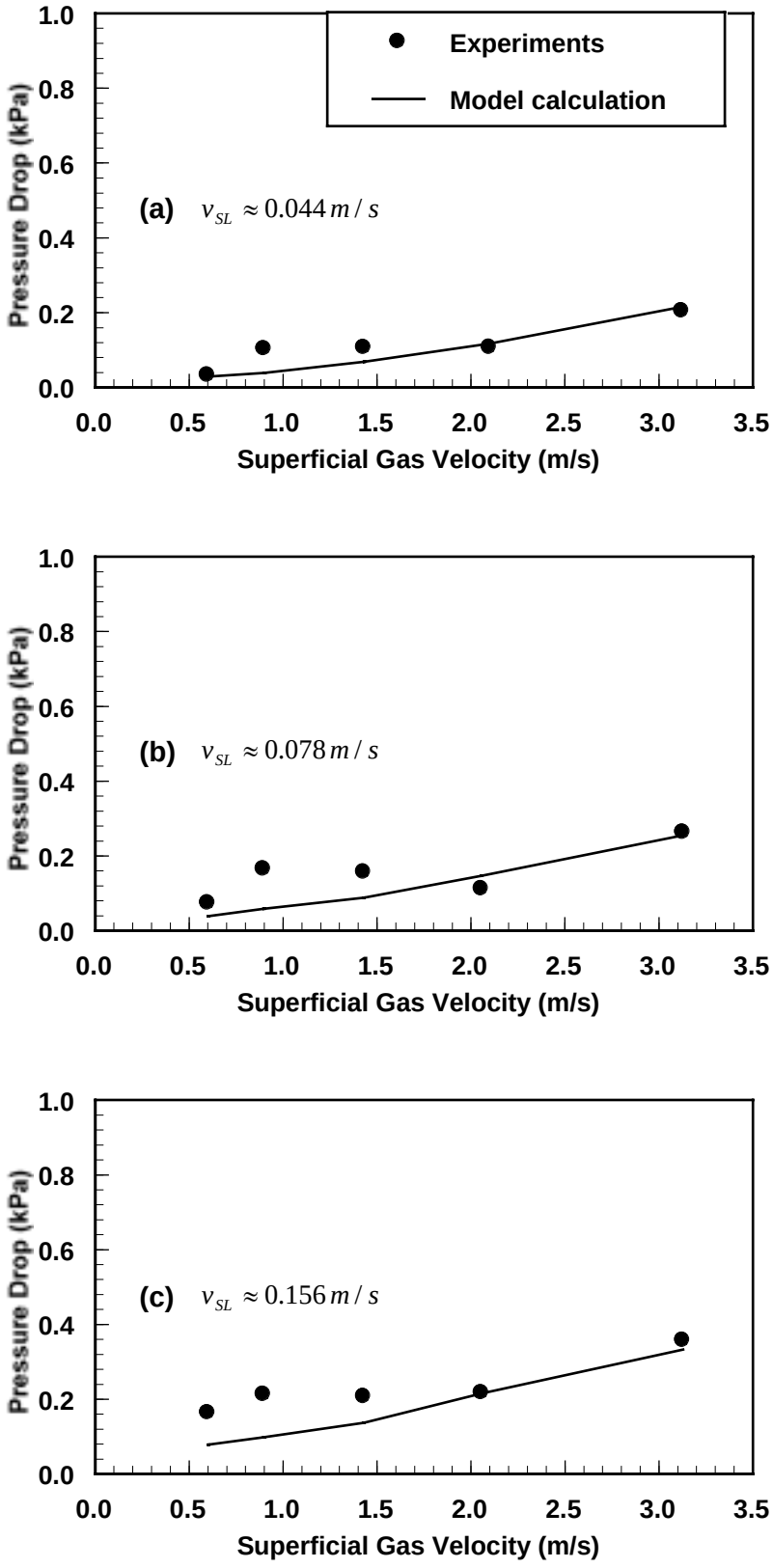

Fig. 5-16 Pressure Drop for 10 m vs. Gas Velocity for Stratified Flow, θ = 0°

The performance of the model for stratified flow of all inclination angles is shown in **Fig. 5-17**. **Fig. 5-17 (a)** shows a comparison between the predicted and measured pressure drops for the low-pressure conditions, and **Fig. 5-17 (b)** for the high-pressure conditions. The predictions of the proposed model resulted in 1.59 % average error, 27.17 % absolute average error, and 44.59 standard deviation for low-pressure conditions, and in -4.21 % average error, 35.81 % absolute average error, and 69.55 standard deviation for high-pressure conditions.

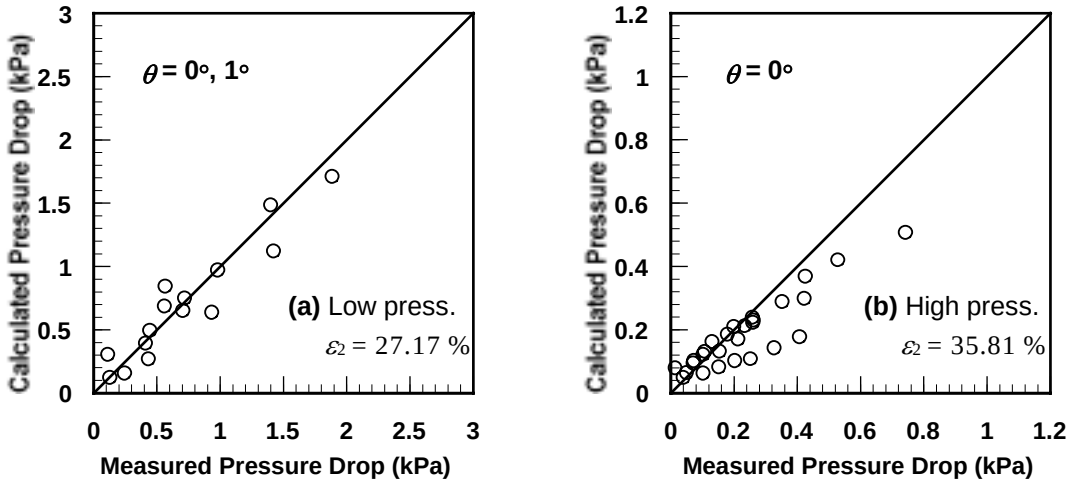

Fig. 5-17 Accuracy of Pressure Drop Calculations for Stratified Flow

5.4.3 Intermittent Flow

For intermittent flow, the same model based on the momentum balance was applied to three flow patterns of elongated-bubble, slug, and froth flow. Calculations for the froth flow were sensitive to the translational velocity used for liquid holdup. **Fig. 5-18** and **Fig. 5-19**, present the performance of the model for intermittent flow at each inclination angle and all angles, respectively.

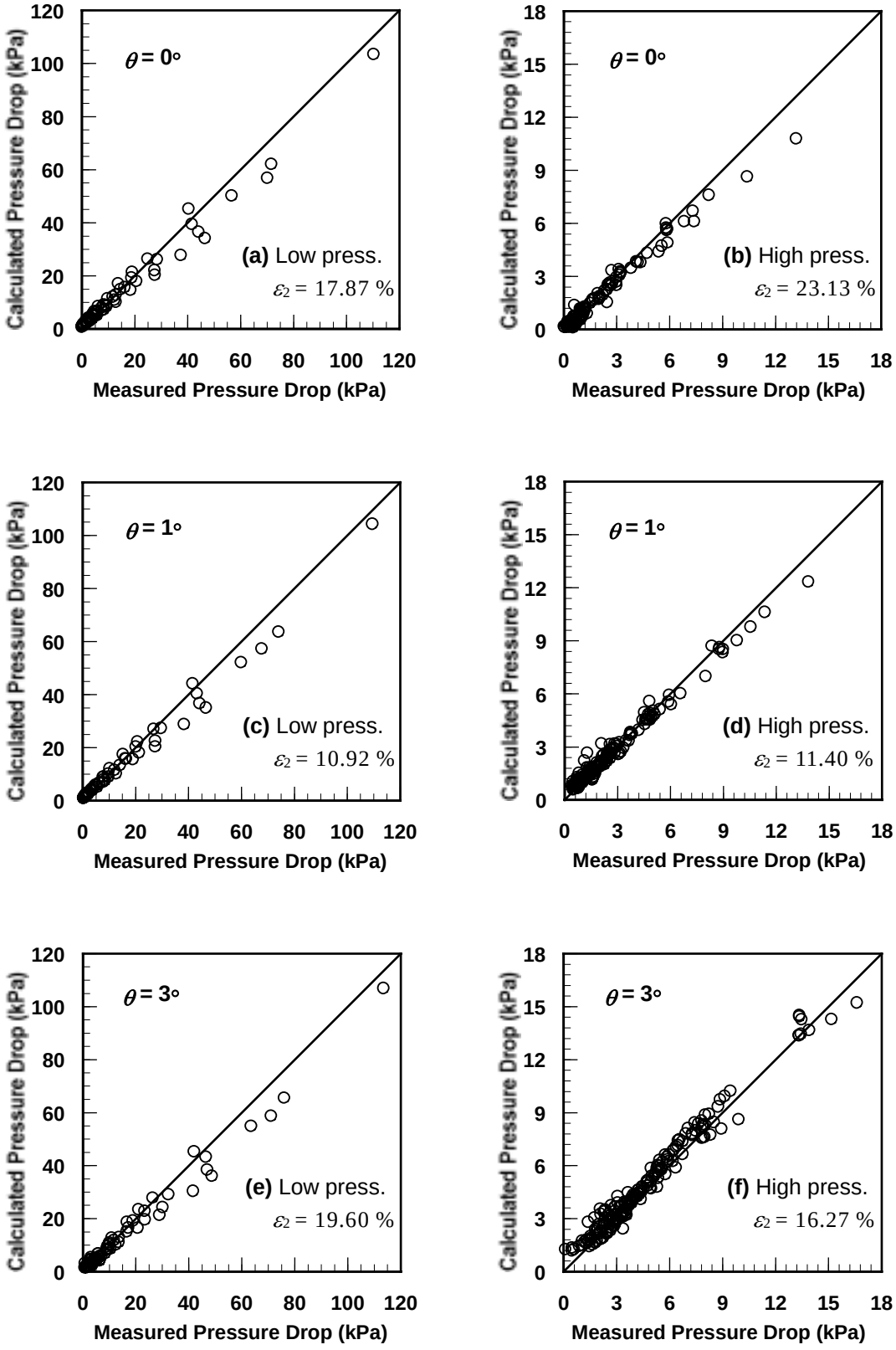

Fig. 5-18 Accuracy of Pressure Drop Calculations for Intermittent Flow at Each Inclination Angle

Fig. 5-19 (a) displays a comparison between the predicted and measured pressure drop of 195 data points for the all inclination angles at low-pressure conditions, and **Fig. 5-19 (b)** shows 467 data points for the all inclination angles at high-pressure conditions. The predictions of the proposed model show good agreements with this data set, with -4.40 % average error, 16.13 % absolute average error, and 21.81 standard deviation for low-pressure conditions, and with 1.04 % average error, 16.02 % absolute average error, and 38.40 standard deviation for high-pressure conditions.

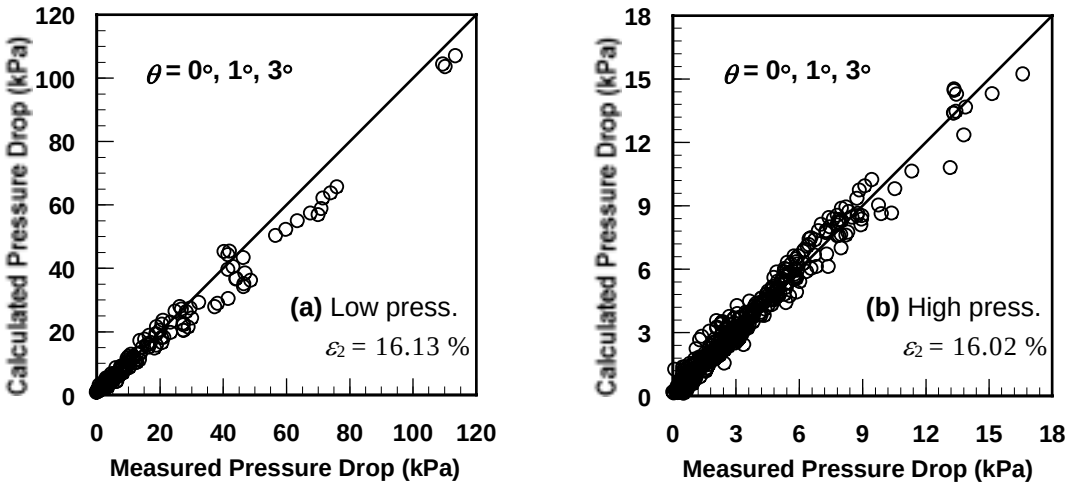

Fig. 5-19 Accuracy of Pressure Drop Calculations for Intermittent Flow of All Inclination Angles

5.4.4 Annular Flow

For the pressure drop prediction of annular flow, the model based on the non-uniform film thickness distributions was used. For correlation of the liquid-wall frictional factor at the bottom and top walls, the use of different Reynolds numbers (Eqs. (4-66) and (4-67)) for liquid-wall friction factor (Eq. (4-15)) in stratified flow proposed by Liang-Biao and Aziz was found more effective to improve accuracy. Predictions of the annular model for pressure drop are plotted against the experimental measurements of 18 data points for all inclination angles as shown in **Fig. 5-20**. The predictions of the proposed model show good agreements with this data set, with -4.91 % average error, 12.15 % absolute average error, and 15.46 standard deviation.

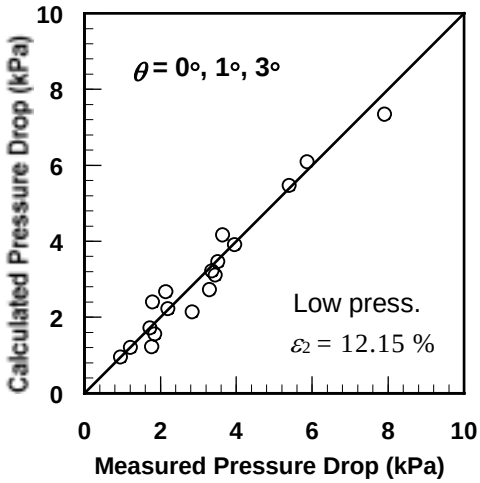

Fig. 5-20 Accuracy of Pressure Drop Calculations for Annular Flow

5-5 Overall Evaluations

5.5.1 Liquid Holdup

Fig. 5-21 displays comparisons between the model calculations and measured liquid holdup for each flow pattern. The predictions of the proposed model show good agreement with this data set, with -0.43 % average error, 2.27 % absolute average error, and 3.37 standard deviation for dispersed bubble flow, with -11.15 % average error, 15.38 % absolute average error, and 16.50 standard deviation for stratified flow, with -5.39 % average error, 8.83 % absolute average error, and 11.51 standard deviation for intermittent flow, with 87.09 % average error, 87.09 % absolute average error, and 25.94 standard deviation for annular flow.

Fig. 5-22 displays comparisons between the model calculations and measured liquid holdup for each inclination angle. The predictions of the proposed model show excellent agreement with this data set, with -2.87 % average error, 11.06 % absolute average error, and 18.43 standard deviation for 0° inclined flow, with -3.79 % average error, 8.55 % absolute average error, and 16.09 standard deviation for 1° inclined flow, and with -3.43 % average error, 8.90 % absolute average error, and 15.76 standard deviation for 3° inclined flow.

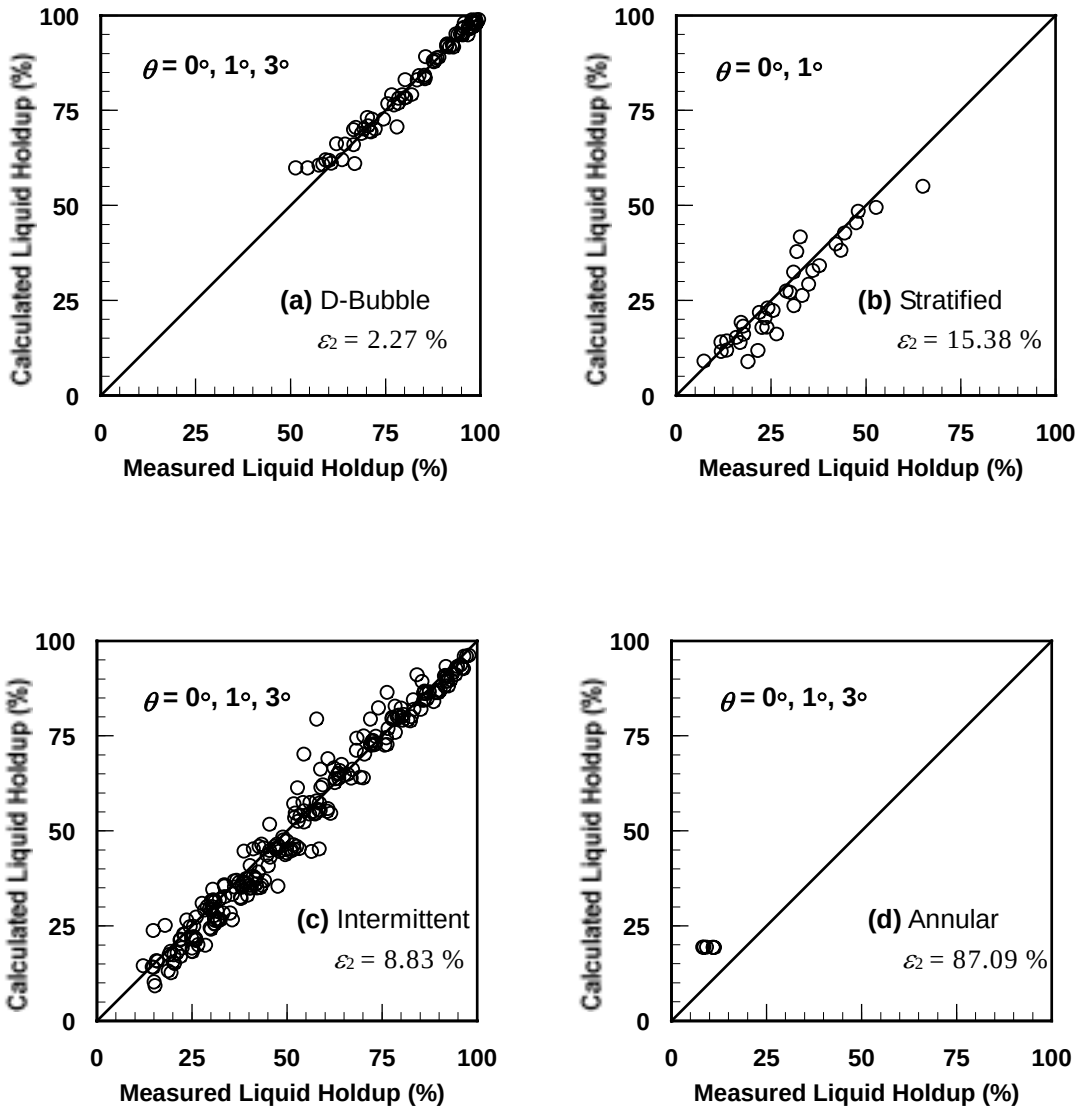

Fig. 5-21 Accuracy of Liquid Holdup Calculations for Each Flow Pattern

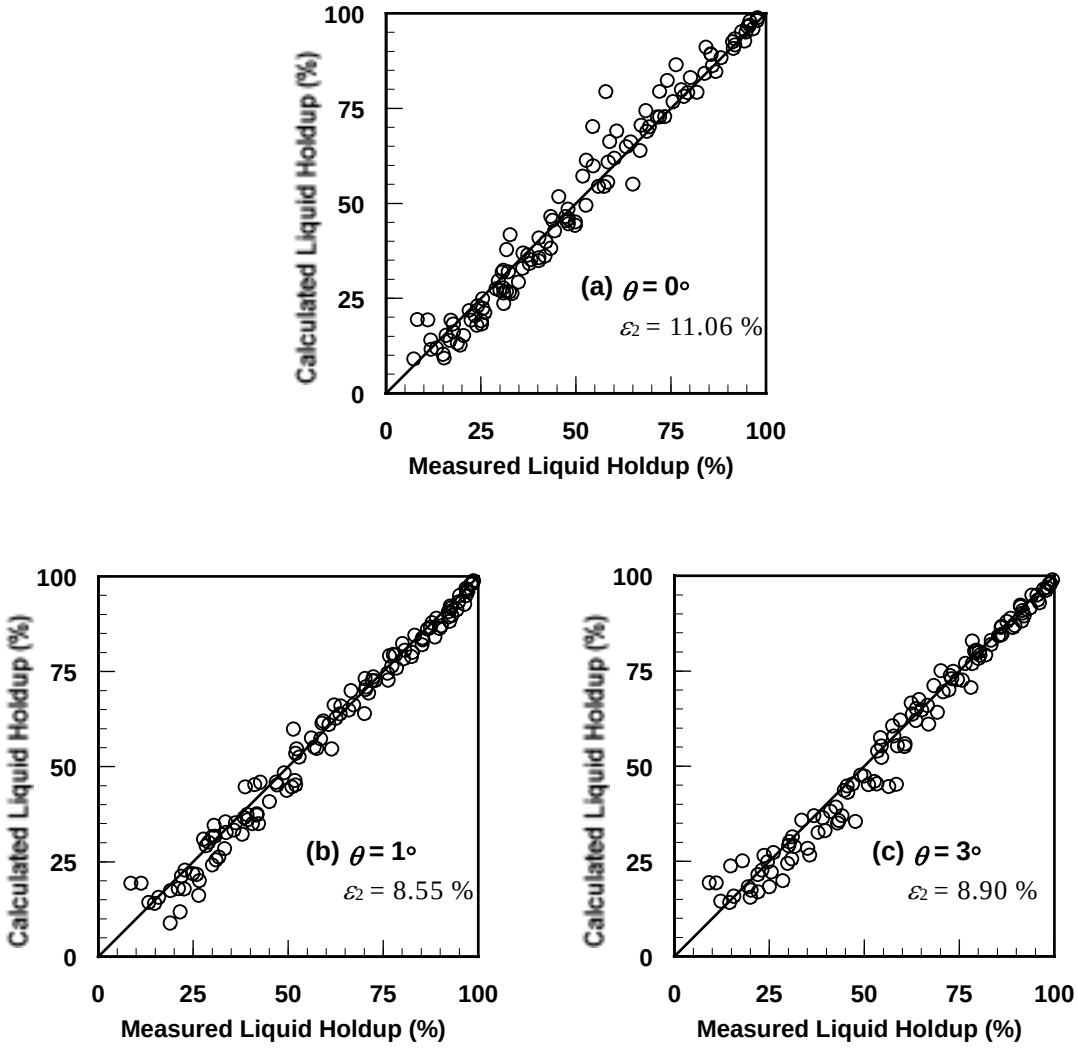

Fig. 5-22 Accuracy of Liquid Holdup Calculations for Each Inclined Flow

5.5.2 Pressure Drop

Fig. 5-23 demonstrates comparisons between the model calculations and measured pressure drop for each flow pattern. The predictions of the proposed model show excellent agreement with this data set, with 3.32 % average error, 5.86 % absolute average error, and 8.09 standard deviation for dispersed bubble flow, with -2.14 % average error, 32.72 % absolute average error, and 61.27 standard deviation for stratified flow, with 0.56 % average error, 16.05 % absolute average error, and 34.43 standard deviation for intermittent flow, with -4.91 % average error, 12.15 % absolute average error, and 15.46 standard deviation for annular flow.

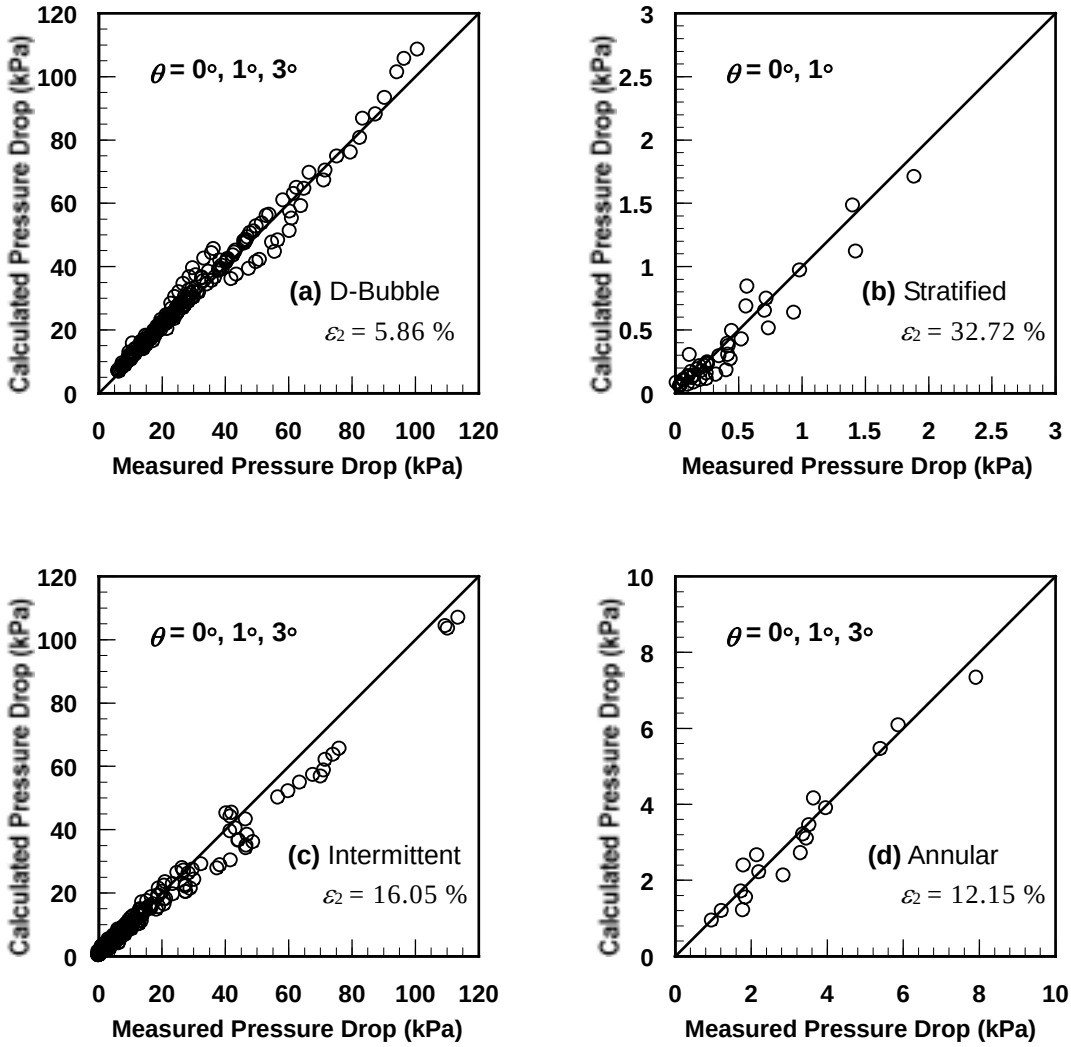

Fig. 5-23 Accuracy of Pressure Drop Calculations for Each Flow Pattern

Fig. 5-24 displays comparisons between the model calculations and measured pressure drop for each inclination angle. The predictions of the proposed model show excellent agreement with this data set, with -5.83 % average error, 19.18 % absolute average error, and 32.79 standard deviation for 0° inclined flow, with 0.74 % average error, 9.88 % absolute average error, and 15.89 standard deviation for 1° inclined flow, and with 4.66 % average error, 14.70 % absolute average error, and 40.91 standard deviation for 3° inclined flow.

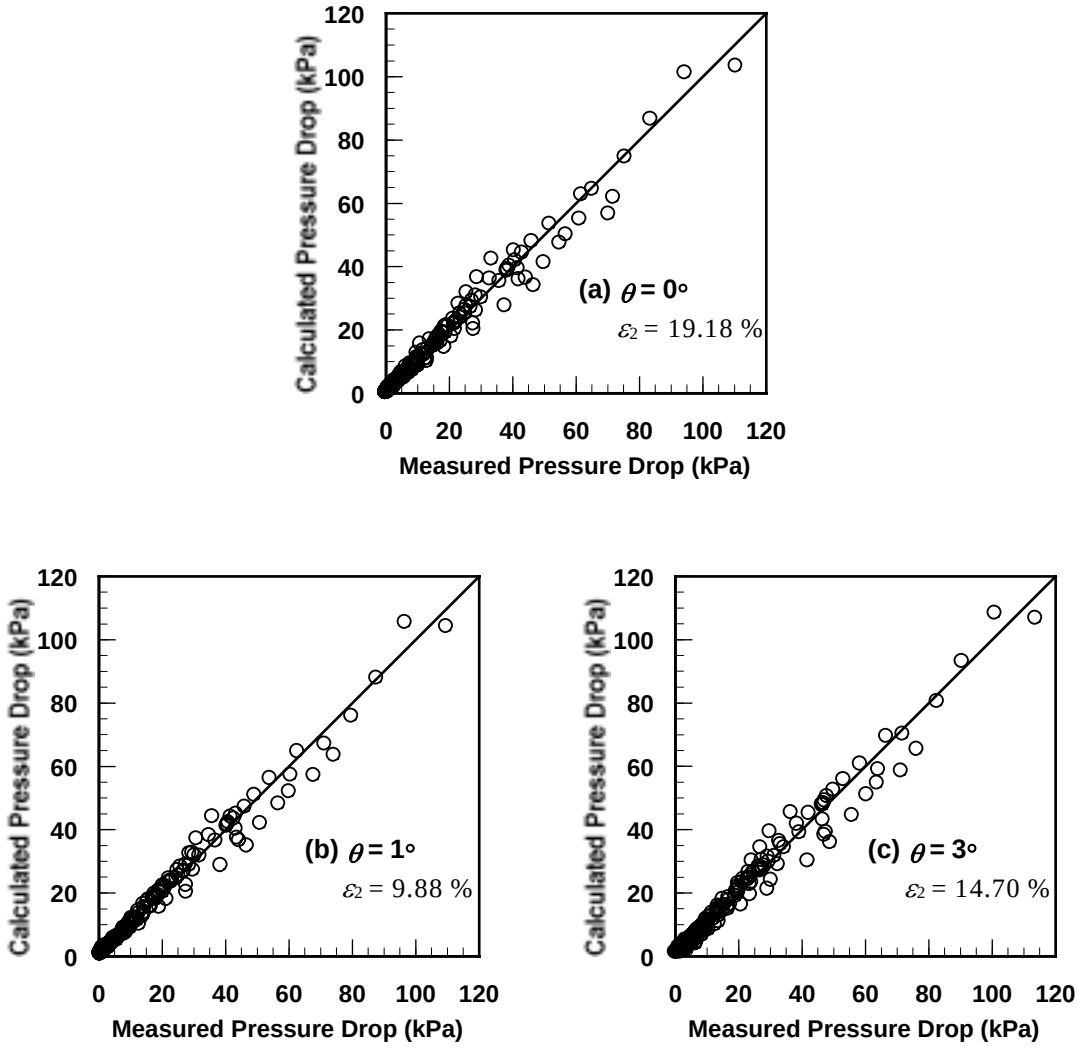

Fig. 5-24 Accuracy of Pressure Drop Calculations for Each Inclined Flow

5.5.3 All Data

The overall performance of the proposed model was evaluated against the total 348 experimental data for liquid holdup and total 938 experimental data for pressure drop as shown in **Table 5-3** and **Fig. 5-25**. For the combined data sets, the proposed model shows an excellent performance for both liquid holdup and pressure drop, with an -3.36 % average error, 9.50 % absolute average error, and 16.76 standard deviation for liquid holdup, and with 0.18 % average error, 14.38 % absolute average error, and 31.99 standard deviation for pressure drop.

Table 5-3 Overall Evaluation of Liquid Holdup and Pressure Drop

Flow patterns	Average error ε_1 [%]	Absolute average error, ε_2 [%]	Standard deviation, ε_3	Number of data
Liquid Holdup				
Dispersed bubble	-0.43	2.27	3.37	72
Stratified	-11.15	15.38	16.50	36
Intermittent	-5.39	8.83	11.51	234
Annular	87.09	87.09	25.94	6
0°	-2.87	11.06	18.43	116
1°	-3.79	8.55	16.09	116
3°	-3.43	8.90	15.76	116
All data	-3.36	9.50	16.76	348
Pressure drop				
Dispersed bubble	3.32	5.86	8.09	216
Stratified	-2.14	32.72	61.27	42
Intermittent	-0.56	16.05	34.43	662
Annular	-4.91	12.15	15.46	18
0°	-5.83	19.18	32.79	280
1°	0.74	9.88	15.89	323
3°	4.66	14.70	40.91	335
All data	0.18	14.38	31.99	938

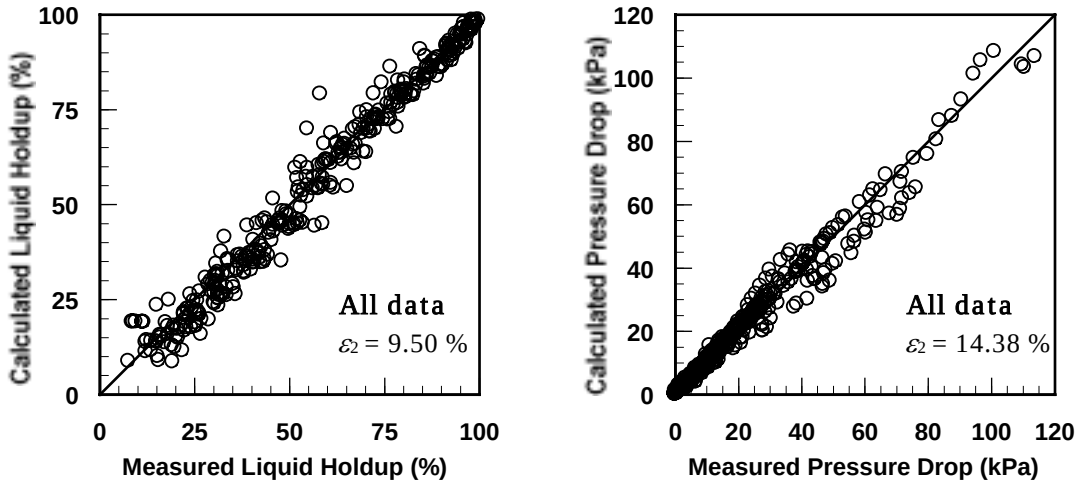

Fig. 5-25 Accuracy of Liquid Holdup and Pressure Drop Calculations for All Data

5.6 Summary

Flow pattern maps were constructed with the results predicted by the proposed model. The predicted flow-pattern boundaries demonstrated good agreements with experimental data.

The overall performance of the new mechanistic model was evaluated against the total 348

experimental data for liquid holdup and total 938 experimental data for pressure drop. The model calculations of liquid holdup and pressure drop presented good agreements with experimental data for each flow pattern and each inclined flow.

References

1) Barnea, D.: “A Unified Model for Predicting Flow-Pattern Transitions for the Whole Range of Pipe Inclinations,” *Int. J. Multiphase Flow*, **13**, (1), 1-12 (1987).

2) Bendiksen, K. H., Espedal, M.: “Onset of Slugging in Horizontal Gas-Liquid Pipe Flow,” *Int. J. Multiphase Flow*, **18**, (2), 237-247 (1992).

3) Taitel, Y. Dukler, A. E.: “A Modeling for Predicting Flow Regime Transition in Horizontal and Near Horizontal Gas-Liquid Flow,” *AIChE Jl*, **22**, (1), 47-54 (1976).

4) Abduvayt, P., Arihara, N., Sharma, Y., Yoshida, Y.: “A Mechanistic Model for Gas-liquid Two-phase Flow in Slightly Inclined pipes: To Improve Prediction of Flow Patterns and Pressure Drop,” *J. Japan Petroleum Institute*, **45**, (3), 175-186 (2002).